 https://doi.org/10.3311/PPch.24008

Periodica Polytechnica Chemical Engineering, 68(3), pp. 338–347, 2024

Effect of Nanophotocatalyst WO_3 Addition on PVDF Membrane Characteristics and Performance

Tutuk Djoko Kusworo[1*], Monica Yulfarida[1], Andri Cahyo Kumoro[1], Dani Puji Utomo[1], Nita Aryanti[1]

[1] Department of Chemical Engineering, Faculty of Engineering, Universitas Diponegoro, Jl. Prof. Sudarto No. 13, Tembalang, 50275 Semarang, Indonesia
[*] Corresponding author, e-mail: tdkusworo@che.undip.ac.id

Received: 04 December 2023, Accepted: 07 May 2024, Published online: 10 July 2024

Abstract

The addition of photocatalyst materials in the membrane has great potential to increase membrane performance and characteristics. In this study, nano photocatalysts WO_3 were added to the polyvinylidene fluoride (PVDF) membrane for process water treatment from rubber industry. The results of SEM and XRD showed the presence of nano photocatalyst WO_3, indicating the successfully embedded nano photocatalyst in PVDF membranes. The addition of nano photocatalyst materials has increased hydrophilicity by increasing the membrane's water uptake ability and decreasing the membrane's contact angle. The PVDF-WO_3-2%wt membrane showed the highest flux value at 64.29 L m^{-2} h^{-1} with 96.40%, 85.61%, and 93.88% of chemical oxygen demand (COD), total dissolved solid (TDS), and ammonia rejection, respectively. The photocatalytic degradation effect of PVDF-WO_3 is proven by a significant difference in the filtration results under vis-light irradiation. Membrane resulted in a better performance in photo-filtration (visible light) than in the dark condition. The PVDF-WO_3-2%wt membrane also showed an excellent reusability after being used for 8 hours of the photo-filtration process. This research is promising to increase the use of photocatalytic membranes in rubber wastewater treatment into clean water.

Keywords

membrane, photocataytic, rubber

1 Introduction

The development of the rubber industry in Indonesia tends to increase significantly, with an average increase of 1.36%. The increment in the rate of rubber production every year is followed by a large amount of waste generated. The wastewater produced has a high concentration of suspended solids, proteins, lipid, inorganic salts, acidic pH (4.2–6.3), 120–15,000 mg L^{-1} of chemical oxygen demand (COD) and 100–9,500 mg L^{-1} ppm of biological oxygen demand (BOD), and 30–525 mg L^{-1} of total suspended solid (TSS) [1]. Indeed, this process water content exceeds their maximum safe level threshold for immediate industrial wastewater disposal.

Several studies have been conducted to treat process water from rubber industry into clean water, such as filtration, coagulation, flocculation, sedimentation, electrodialysis, and advanced oxidation processes [2–4]. Among these methods, membrane technology is one of the effective methods for wastewater treatment. Membrane technology does not require additional chemicals during the filtration process, has a wide separation range, high-efficiency process, and has become a compelling method for wastewater treatment [5]. Membrane technology for process water treatment from rubber industry has been carried out by many previous researchers and currently continues to be developed. The main problem in the use of membranes is the occurrence of membrane fouling [6]. Membranes can be fabricated from several polymers, such as polyvinylidene fluoride (PVDF), polysulfone (PSf), and polyethersulfone (PES). Among these, PVDF has several advantages over other polymers, with high mechanical strength and excellent chemical resistance. The polymer can be modified to increase its hydrophilicity and minimize the presence of fouling on the membrane. Various modification methods, such as adding additives to the membrane or a hybrid membrane [7], can be done. Hybrid membranes can be made by blending the nanoparticles into the polymer to increase membrane absorption or diffusion capacity [8].

Previous studies have shown that hydrophilic nanomaterials blending is a practical modification process to improve the antifouling performance of membranes [9].

Cite this article as: Kusworo, T. D., Yulfarida, M., Kumoro, A. C., Utomo, D. P., Aryanti, N. "Effect of Nanophotocatalyst WO_3 Addition on PVDF Membrane Characteristics and Performance", Periodica Polytechnica Chemical Engineering, 68(3), pp. 338–347, 2024. https://doi.org/10.3311/PPch.24008

In recent studies, photocatalytic materials are being developed due to their ability to increase membrane performance through the photocatalytic degradation process. The addition of photocatalytic material can increase the membrane's ability to remove organic pollutants in process water from rubber industry, thereby reducing the fouling development [10]. Tungsten oxide (WO_3) and molybdenum disulfide were reported as promising photocatalysts with lower band gap and sensitivity to visible light [11, 12]. WO_3 material, which has a narrow band gap value range (~2.7 eV), can be combined with MoS_2, which has an almost equal band gap energy, to form heterojunctions [12]. Several studies have been conducted using WO_3 for degrading pollutants in wastewater. In the research by Singla [13], MoS_2/WO_3 nanophotocatalyst material showed good performance in organic pollutants degradation with 80% COD rejection. In visible light, photocatalytic nano photocatalyst materials can produce radicals to degrade the organic pollutants contained in wastewater [14]. These promising results indicate that the WO_3 photocatalytic nano photocatalyst has the potential to be a superb nanoparticle selection for better membrane characteristics and performance for wastewater treatment. However, the WO_3 photocatalyst was only used directly for wastewater treatment, and the blending of photocatalytic materials into the membrane, which has great potential, has not been widely studied.

To our knowledge, this is the first study combining WO_3 photocatalyst with PVDF membrane. The addition of photocatalytic nanophotocatalysts on membranes has good potential, especially in the membrane performance through a combination of physical separation through filtration, and photocatalytic degradation has not been studied in depth. The study of permeability and rejection efficiency parameters is significant to determine the influence of the addition of the nano photocatalyst WO_3 on membrane characteristics and performance. Moreover, photocatalytic nano photocatalysts may be increased the mechanical strength of the membrane to prolong the durability of modified membranes.

2 Materials and methods

2.1 Materials

PVDF powder was bought from Solvay Advanced Materials, USA. N-Methyl-2-pyrrolidone (NMP) was supplied from Merck, Indonesia. WO_3 (powder, 50 nm) was bought from Shanghai Chemicals Ltd, China, and used as received. A sample of process water from rubber industry was obtained from the effluent stream of the industrial PTPN VII, Bengkulu.

2.2 Fabrication of PVDF-WO_3 membrane

The PVDF-WO_3 membrane was prepared using the dry-wet non-solvent induced phase inversion (NIPS) method. specific amount of WO_3 was added to the total solid with a concentration of 1%wt and 2%wt. The nano photocatalyst was first mixed with NMP and sonicated for 1 h. The specific amount of PVDF powder (15%wt) was dissolved using NMP solvent and stirred for 1 h using a stirrer at 60 °C until homogeneous. The nano photocatalyst was mixed into the dope solution, stirred for 7 h at 60 °C and degassed for 24 h. The solution was then cast on a clean glass plate using a casting knife with a thickness of 0.15 mm. The casted membrane was then immersed in a coagulation bath filled with deionized water for 24 h and then dried for 24 h.

2.3 Characterization of process water from rubber industry

The initial characterization of process water from rubber industry consists of physical appearance, odor, and COD concentration tested by redox titration, total dissolved solid (TDS) concentration tested with TDS meter A-013, China, and nitrogen content tested with Nessler reagent using a UV-Vis spectrophotometer. The initial characteristics of process water from rubber industry to be treated are presented in Table 1.

2.4 Characterization of fabricated membrane

The top surface morphology of the membrane was analyzed using scanning electron microscopy (SEM) (JSM-6510-LA, JEOL, Tokyo, Japan) at 1000× magnification. Membrane crystallinity was analyzed using X-ray diffraction (XRD) (Panalytical Xpert Pro MPD, Netherlands) at diffraction angles ranging from 10° to 80°. The membrane's mechanical properties were analyzed using a material testing machine (UTS H001, China) by measuring the tensile strength and elongation break values. The hydrophilicity

Table 1 Initial characteristic of process water from rubber industry

Parameter	Unit	Value
Apperance	–	Yellowish
COD	ppm	900 ± 5.32
TDS	ppm	4000 ± 7.54
Ammonia	ppm	289 ± 3.45

of the membrane surface was analyzed by measuring the membrane contact angle using a water contact angle meter (RASE contact angle meter, Japan).

2.5 Water uptake ability of the membrane

Water uptake ability was measured using Eq. (1):

$$U = \frac{w_w - w_d}{w_d} \cdot 100\%, \tag{1}$$

where U is the water uptake ability (%), w_w and w_d are the wet and dry weights of the membrane, respectively (g).

2.6 Membrane porosity

The porosity measurement of the membrane was carried out by immersing the membrane for 24 h in distilled water. Then the membranes were placed in a vacuum oven for 24 h at 60 °C. The membrane porosity was calculated using Eq. (2):

$$\varepsilon = \frac{w_w - w_d}{\rho_w \cdot A \cdot \delta}, \tag{2}$$

where ε is the membrane porosity (%), ρ_w is the density of pure water at ambient condition (0.997 g cm^{-3}), A is the membrane surface area (cm^{-2}), and δ is the thickness of the membrane (cm). The average pore radius was analyzed using the Guerout-Elford-Ferry approximation using Eq. (3):

$$r = \sqrt{\frac{8 \cdot \eta \cdot \delta \cdot Q \cdot (2.9 - 1.75 \cdot \varepsilon)}{\varepsilon \cdot A \cdot \Delta P}}, \tag{3}$$

where η is the pure water viscosity at ambient condition (8.9×10^{-4} Pa·s), δ is the membrane thickness (m), Q is the permeate volumetric flow rate (m^3 s^{-1}), and ΔP is the transmembrane pressure (Pa).

2.7 Membrane performance

The membrane separation process is carried out with a cross-flow system shown in Fig. 1. Process water from rubber industry without pre-treatment was used as a feed and passed through a module with a 12.57 cm^2 membrane using 5 bar operating pressure. The filtration was conducted in dark and light conditions using visible light irradiation [15].

Permeate flux of each membrane was recorded every 30 min for 5 h using Eq. (4):

$$J = \frac{\Delta V}{A \cdot \Delta t}, \tag{4}$$

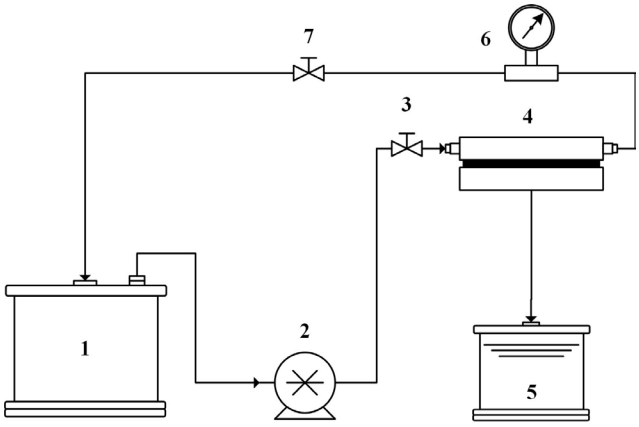

Fig. 1 Membrane cross filtration system

where J is the permeate flux (L m^{-2} h^{-1}), ΔV is the permeate volume (L), A is the effective membrane area (m^2), and Δt is the filtration time (h).

The main parameters in membrane selectivity assessing pollutant rejection were seen from the concentration of COD, TDS, and ammonia before and after the membrane filtration process. The rejection was calculated using Eq. (5):

$$R = \left(1 - \frac{c_p}{c_f}\right) \cdot 100\%, \tag{5}$$

where R is rejection efficiency (%), c_p and c_f are the pollutant concentrations in permeate and feed solution, respectively (mg L^{-1}).

The antifouling properties of the membrane were evaluated using flux recovery ratio (*FRR*), total fouling ratio (R_t), reversible fouling ratio (R_r), and irreversible fouling ratio (R_{ir}) by using Eqs. (6)–(9) [16]:

$$FRR = \left(\frac{J_1}{J_0}\right) \cdot 100\%, \tag{6}$$

$$R_t = \left(\frac{J_0 - J_2}{J_0}\right) \cdot 100\%, \tag{7}$$

$$R_r = \left(\frac{J_1 - J_2}{J_0}\right) \cdot 100\%, \tag{8}$$

$$R_{ir} = \left(\frac{J_0 - J_1}{J_0}\right) \cdot 100\%, \tag{9}$$

where J_0 is the initial pure water flux, J_1 is the final pure water flux after the cleaning process, and J_2 is the permeate flux (L m^{-2} h^{-1}).

3 Result and discussion

3.1 Membrane performance

3.1.1 Surface morphological study

The morphological characteristics of membranes are used to support membrane performance analysis on permeability and selectivity. The effect of WO_3 addition can be seen from the different results on the top surface of neat PVDF and PVDF-WO_3 membrane, as seen in Fig. 2.

In Fig. 2 (a), the neat PVDF membrane shows some defects due to the non-concurrent compaction of the membrane during the coagulation process [17]. In Fig. 2 (b), the addition of the WO_3 does not cause any defect, as seen in the neat PVDF membrane, but there are some white spots on the surface. The white spot indicates the presence of WO_3 on the membrane. It also indicates the incomplete dispersion of the nano photocatalyst on the membrane, so it causes agglomerates to form on the membrane surface as marked with the white dots [18]. However, there are not many white dots on the membrane surface, so it can be seen that there are more nanomaterial WO_3 that has been successfully embedded into both the membrane surface and pores.

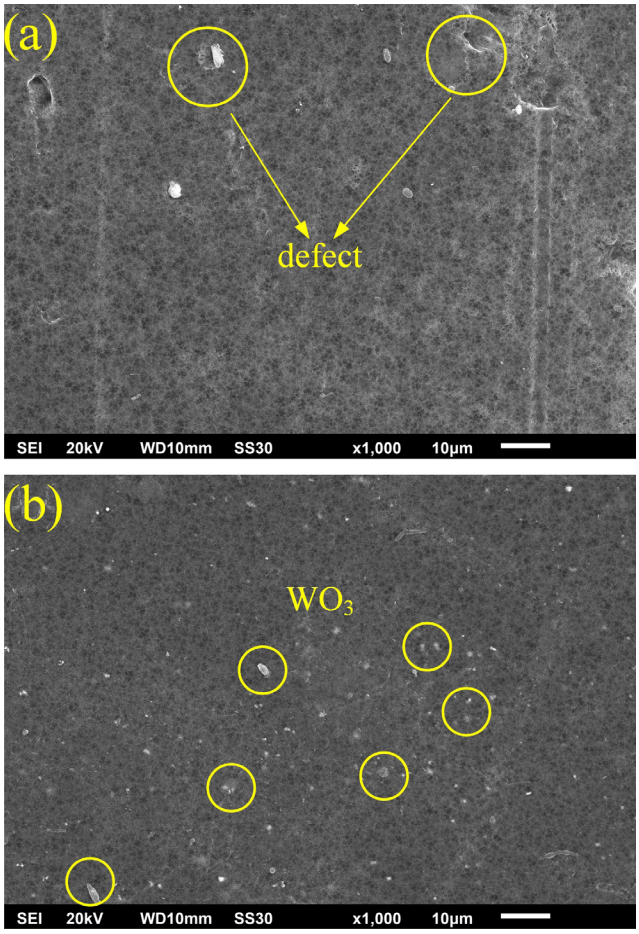

Fig. 2 Surface morphology of (a) neat PVDF and (b) PVDF-WO_3

3.1.2 Membrane functional group and structural analysis

The chemical function group of the membrane was analyzed using FTIR, and the structural crystallinity of the membrane was analyzed using XRD. The results of the FTIR analysis were carried out on neat PVDF and PVDF-WO_3 membranes, and the result was depicted in Fig. 3 (a).

In Fig 3 (a), several strong peaks can be seen on the neat PVDF membrane, which is a peak at 970 cm^{-1}, which indicates the stretching of –C–O–C– functional groups, the peak at 1203 cm^{-1}, which indicates asymmetric stretching of the CF2 bond and at 1490 cm^{-1} which indicates the CH bonding [19]. The addition of WO_3 material shows some new peaks at 609 cm^{-1}, indicating O-W-O, and 759 cm^{-1}, indicating the W-O-W bond. The two peaks indicate the chemical bond between the PVDF polymer and WO_3 material. Through these expected results, it is proven that WO_3 material is successfully embedded in the PVDF membrane. In Fig. 3 (b), the neat PVDF membrane has a semi-amorphous structure with little peaks found at

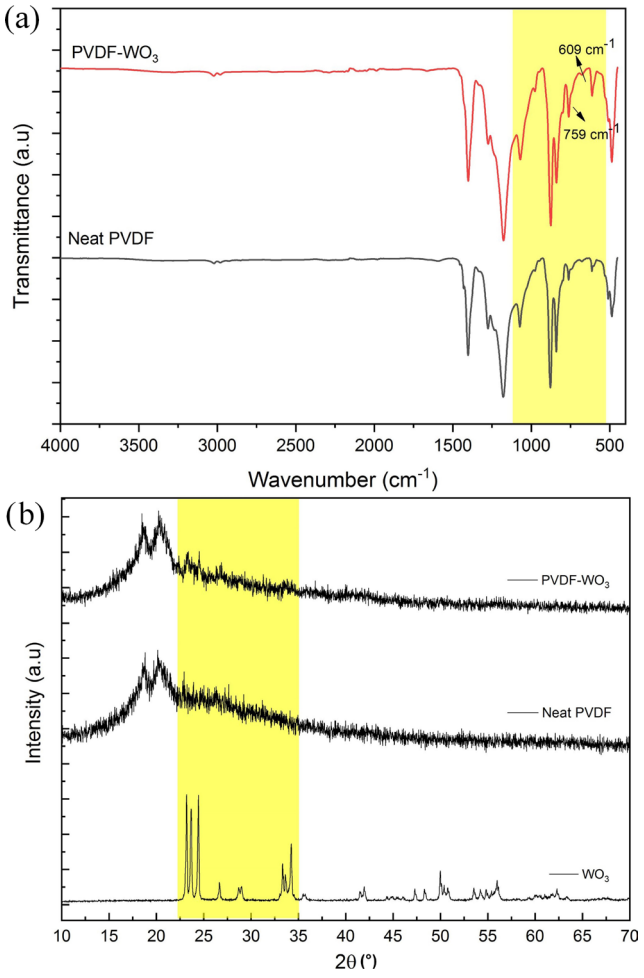

Fig. 3 The result of (a) FTIR and (b) XRD of fabricated membrane

18.80° and 20.40° [20]. In contrast, the nano photocatalyst WO_3 has a crystal structure with several sharp peaks at 23.20°, 33.32°, 34.24°, 53.54°, 62.32°, and 77.02°. The diffractogram of the PVDF-WO_3 membrane showed a similar result to the neat PVDF membrane, with several sharp peaks at 23.26°, 24.52°, and 79.76°. Some of these peaks indicate the nano photocatalyst WO_3 on the membrane. The XRD and SEM analysis show that the nano photocatalyst was successfully embedded in the membrane.

3.1.3 Pore properties

The pore properties of the membrane are presented in several parameters, such as porosity, pore size, and membrane thickness. The comprehensive data of the parameters can be seen in Table 2.

In Table 2, it can be seen that the thickness of the membrane increases along with the addition of nano photocatalysts. According to the research conducted by Struzyńska-Piron et al. [21], the thickness of the membrane affects the value of the membrane resistance and performance. In the PVDF-WO_3-1wt% membrane, the increment of thickness is not too much and tends to be small so that later it will not significantly reduce the performance of the membrane.

The PVDF-WO_3 membrane has the highest porosity and pore size values among other membranes. Adding nano photocatalyst materials to the membrane increases the formation of pores on the membrane. These results can be correlated with the results of the SEM image in Fig. 2. The increase in pore size affects the flux value and membrane selectivity. Membranes with large pores cause an increase in the value of the membrane flux but decrease the membrane's selectivity. The three fabricated membranes have pore size values that are still included in the ultrafiltration range of 10–100 nm.

3.1.4 Mechanical strength study

A study on mechanical strength is done by evaluating the value of tensile strength and elongation break. The effect of nano photocatalyst addition to the membrane on these two parameters can be seen in Table 3.

The characterization showed that the nano photocatalyst WO_3 was successfully embedded in the membrane.

Table 2 Porosity and average pore size of the fabricated membrane

Membrane	Porosity (%)	Average pore size (nm)
Neat PVDF	27.27 ± 0.70	16.49 ± 1.21
PVDF-WO_3-1%wt	37.03 ± 0.15	17.15 ± 0.73
PVDF-WO_3-2%wt	38.74 ± 0.40	18.23 ± 0.24

Table 3 Porosity and average pore size of the fabricated membrane

Membrane	Thickness (μm)	Tensile strength (Pa)	Elongation at break (%)
Neat PVDF	66.00 ± 0.33	4.88 ± 0.24	11.10 ± 0.56
PVDF-WO_3-1%wt	80.00 ± 0.40	3.62 ± 0.18	11.20 ± 0.55
PVDF-WO_3-2%wt	82.00 ± 0.41	3.64 ± 0.18	11.30 ± 0.57

In Table 3, it can be seen that the addition of nano photocatalysts with several concentrations to the membrane significantly affects the mechanical strength of the membrane. Increasing nano photocatalyst concentration causes the tensile strength and elongation break values to increase. The PVDF-WO_3-2%wt membrane obtained the highest value with a 3.64 kg m^{-2} of tensile strength and 11.30% elongation break. Both parameters are critical because the membrane operates in a pressurized system. The addition of nano photocatalyst to the membrane causes a decrease in the mechanical strength of the membrane. This may be caused by the creation of gaps between the polymer matrix due to the addition of nanoparticles. As more and more gaps are created in the membrane body, the polymer matrix becomes less elastic and more brittle so that its mechanical strength decreases [22].

3.1.5 Hydrophilicity of membrane

The membrane hydrophilicity can be evaluated by the membrane's contact angle, water uptake ability, and pure water flux (PWF) analysis. The hydrophilicity of the membrane will affect the ability of the membrane to absorb water. The effect of nano photocatalyst WO_3 addition on the membrane's hydrophilicity can be seen in Fig. 4.

In Fig. 4 (a), the highest contact angle value is on the PVDF-WO_3-2%wt membrane with a 73.13° contact angle. The decrease of contact angle affects increasing the hydrophilicity of the membrane. The addition of nanoparticles to the membrane can increase the hydrophilicity of the membrane by the presence of dipole-dipole interactions between water and the membrane surface. This interaction causes an increase in the membrane's absorption ability.

In Fig. 4 (b), the PWF increases with the addition of the nano photocatalyst concentration. These results correlate with the contact angle and membrane water uptake ability test results. The addition of WO_3 causes a decrease in contact angle and an increase in water uptake ability, indicating an increase in the hydrophilicity of the membrane. The addition of nano photocatalysts to the membrane causes the membrane to have high availability of hydrophilic sites, increasing the absorption ability. The oxygen

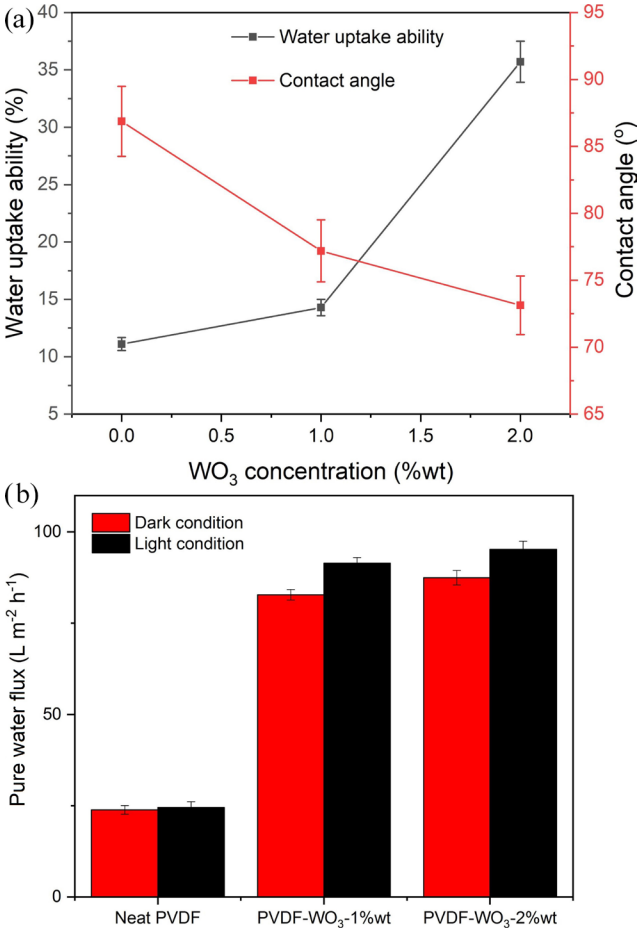

Fig. 4 The result of (a) contact angle and water uptake ability and (b) PWF of fabricated membrane

vacancies exist in the photocatalytic materials could bind and react with water molecules and subsequently generate OH groups. Therefore, hydrophilicity of the photocatalytic materials embedded membranes increased [23]. In addition, the PWF of the membrane with the addition of WO_3 material showed better results in the presence of visible-light irradiation. This is related to the addition of WO_3, a photocatalyst material responsive to visible-light irradiation. The highest PWF value reached 95.22 L m^{-2} h^{-1} on the PVDF-WO_3-2%wt membrane.

3.2 Membrane performance

3.2.1 Permeability

The permeate flux of the membrane was evaluated by the membrane filtration process for 6 h and periodically every 30 min. Photo-filtration tests were carried out in dark and light conditions to see the effect of using photocatalytic nano photocatalysts on visible irradiation. The addition of WO_3 material resulted in a more stable normalized flux in light conditions than in dark conditions. This proves that WO_3 influences the permeability of the membrane under visible-light irradiation. To find out more about the effect of WO_3 on permeability, permeate flux analysis was carried out in two conditions.

In Fig. 5 (a), the neat PVDF membrane shows the lowest initial flux value, 30.20 L m^{-2} h^{-1}. There is no difference in neat PVDF membranes in dark and light conditions. The different results were obtained with the addition of nano photocatalyst WO_3. In the light condition, nano photocatalyst addition causes the initial flux value to be higher and more stable than the dark filtration process due to the photocatalytic activity. The photocatalytic properties of the membrane can minimize fouling so that the flux value of the membrane is higher and stable. The addition of nano photocatalysts showed a better initial flux value, 44.67 L m^{-2} h^{-1}, in dark conditions. There was a significant increase in the initial flux value with adding a nano photocatalyst with vis-light irradiation, as seen in Fig. 5 (b). photocatalyst was successfully

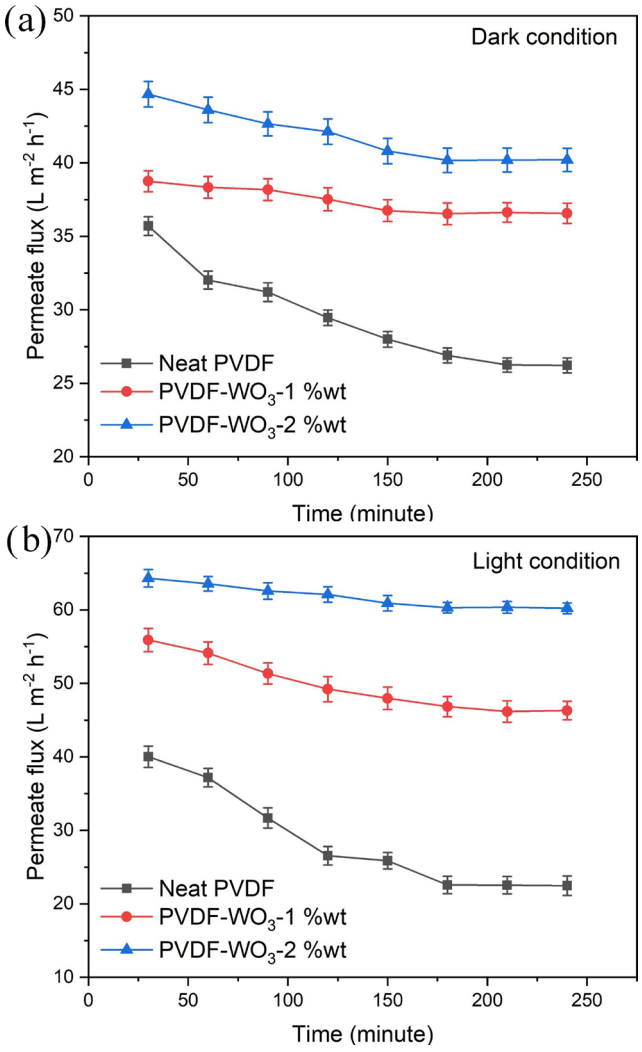

Fig. 5 Permeate flux in (a) dark and (b) light condition

embedded in the membrane. Under vis-light irradiation, PVDF-WO_3-2%wt membrane showed the best performance with 64.29 L m^{-2} h^{-1} of initial permeate flux. The nano photocatalyst has a significant effect on membrane permeability.

3.2.2 Pollutant rejection

The membrane selectivity was examined by evaluating the rejection of pollutants through COD, TDS, and ammonia concentrations in the feed and permeate. In Fig. 6, it can be seen that the neat PVDF membrane has the lowest rejection value, with a 59.17% of COD rejection. The highest pollutant rejection was obtained by PVDF-WO_3-2%wt membrane in light condition, as depicted in Fig. 6 (b). As the results obtained on permeate flux values, the WO_3 nano photocatalyst has an essential role in pollutant degradation. The presence of photocatalytic materials can be degraded the organic pollutants in process water from rubber industry by converting them into CO_2 and H_2O [24]. The use of photocatalytic materials allows the membrane to physically separate pollutants through filtration and is assisted by photocatalytic degradation. The hydrophilicity of the membrane also plays an essential role in pollutant rejection.

The nano photocatalyst added to the membrane produces a hydrophilic layer that can help repel hydrophobic pollutants and produce a positive electrostatic charge, forming a positive layer on the membrane surface [25]. However, the excess nano photocatalyst addition results in a decrease in membrane performance with damage to the membrane pore due to agglomeration resulting in a decrease in membrane selectivity.

3.2.3 Membrane antifouling and reusability

The antifouling properties of the membrane can be analyzed using the R_t, R_r, and R_{ir} values of the membrane. In Fig. 7 (a), it can be seen that the neat PVDF membrane has the highest total fouling (R_t). This indicates that the presence of WO_3 on the membrane has succeeded in increasing the antifouling potential on the membrane surface.

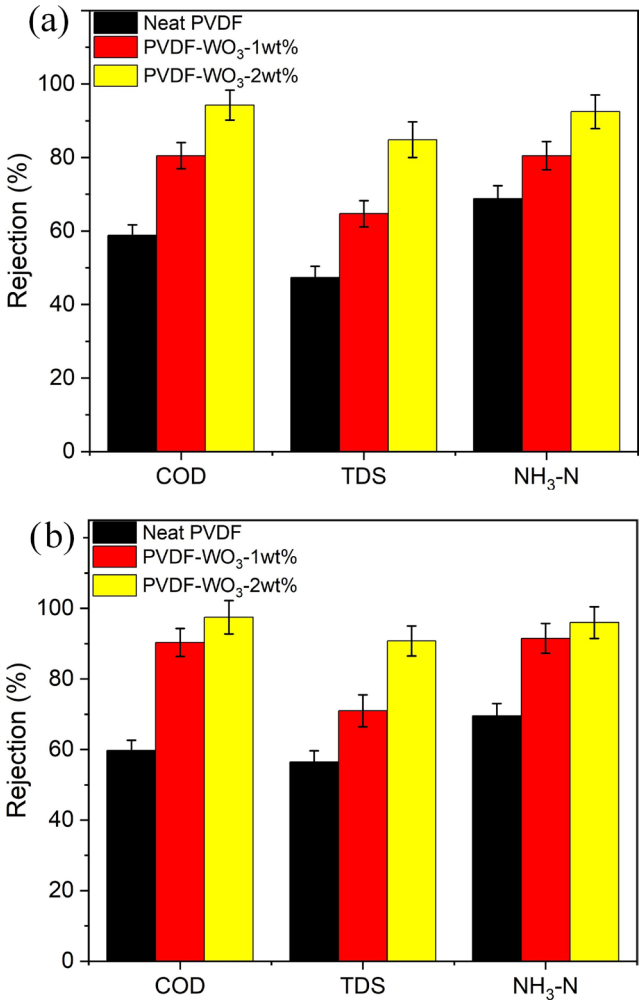

Fig. 6 Pollutant rejection in (a) dark and (b) light condition

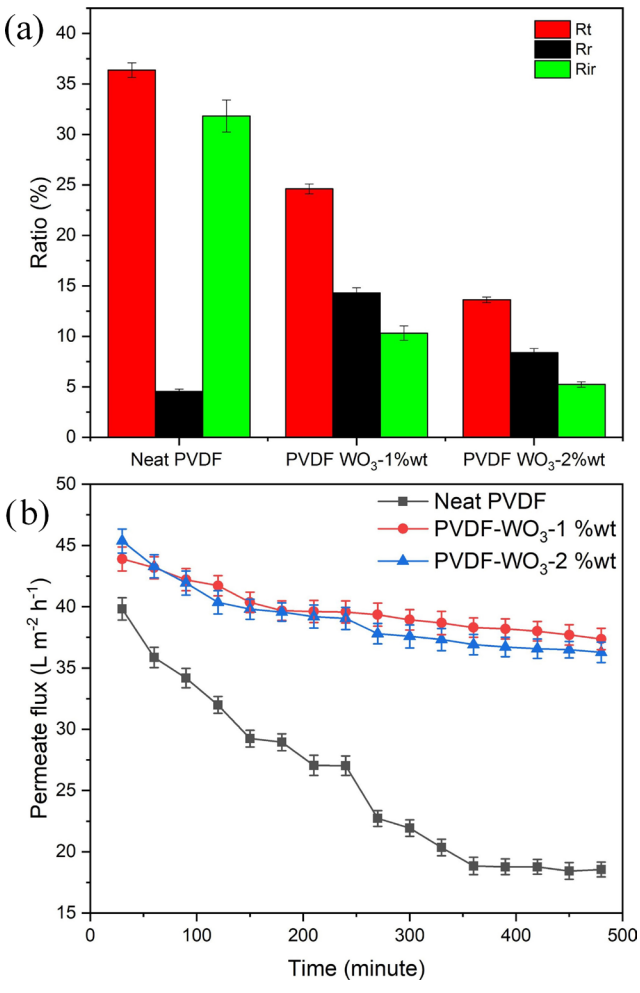

Fig. 7 The result of (a) fouling ratio and (b) reusability test

The PVDF-WO_3 membrane also shows an irreversible fouling ratio less than the reversible fouling ratio (R_r). This is in line with the *FRR* results obtained by the membrane, where increasing the *FRR* indicates less effort is being made to perform hydraulic cleaning on the membrane [26]. This is also supported by the results of the membrane durability test that has been used for 8 h which shows a stable flux on the PVDF-WO_3-2%wt membrane. These results prove that the membrane has good durability for long-term use. The excellent result obtained by the PVDF-WO_3-2%wt membrane shows the success of the WO_3 material in increasing the hydrophilicity, permeability, selectivity, and antifouling properties of the PVDF membrane.

The SEM images presented in Fig. 8 provide valuable insights into the morphological characteristics of the PVDF-WO_3 membranes post-filtration, with and without UV irradiation. Fig. 8 (a) depicts the morphology of the membrane after filtration without UV exposure, revealing significant fouling deposits on the membrane surface. These foulants, consisting of organic and inorganic substances present in the feed solution, adhere to the membrane pores and surfaces, thereby impeding water flow and reducing filtration efficiency. The observed foulant accumulation underscores the susceptibility of PVDF-WO_3 membranes to fouling during practical filtration operations.

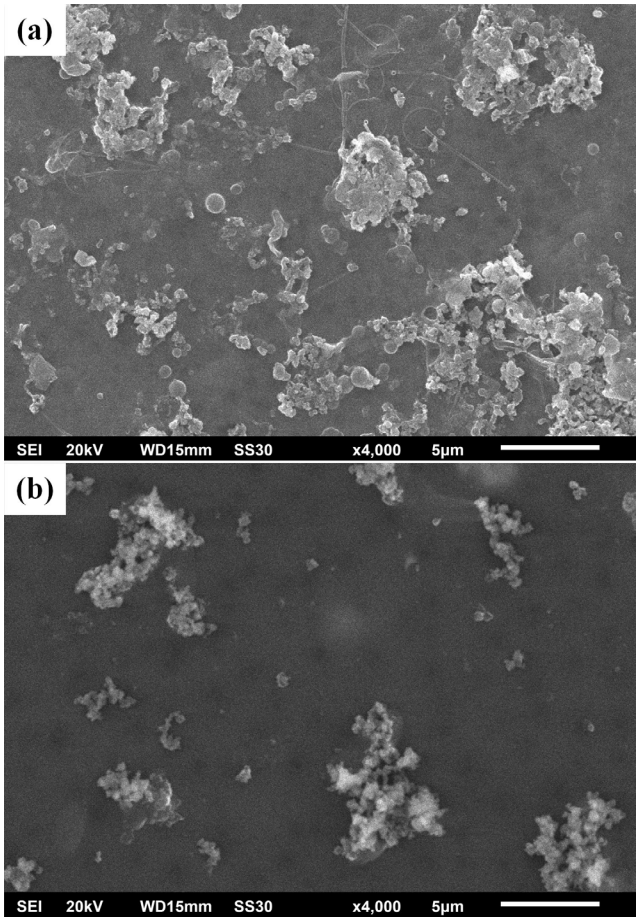

Fig. 8 Surface morphologies of PVDF-WO_3 membrane after filtration (a) without UV irradiation (b) with UV irradiation

Conversely, Fig. 8 (b) illustrates the morphology of the membrane subjected to UV irradiation following filtration. Remarkably, the membrane surface appears significantly cleaner compared to its non-irradiated counterpart. The reduced fouling deposition suggests that UV irradiation exerts a mitigating effect on membrane fouling, possibly through the degradation of organic foulants or enhanced fouling resistance imparted by the photodegradation of foulants. These findings align with previous studies demonstrating the efficacy of UV irradiation in fouling mitigation across various membrane materials [27].

One notable observation from Fig. 8 (b) is the absence of any discernible damage or degradation to the PVDF-WO_3 membrane structure following UV irradiation. This suggests that the applied UV dosage does not induce significant polymer degradation or compromise the structural integrity of the membrane. Such findings are crucial for assessing the feasibility of photocatalytic-based fouling control strategies in practical membrane filtration systems, as membrane durability and stability are paramount for long-term performance.

4 Conclusion

In this study, the PVDF membrane was modified by adding nano photocatalyst WO_3 to improve the membrane performance, as seen from the flux and rejection values. The filtration process using a photocatalytic membrane was carried out in two conditions, dark and light, to see the effect of using nano photocatalyst WO_3, which has photocatalyst properties, to degrade the organic pollutant in process water from rubber industry. The addition of nano photocatalysts produced membranes with better characteristics and performance than PVDF membranes. PVDF-WO_3-2%wt membrane became the membrane with the best characteristics and the best performance in flux values and pollutant rejection. The use of nano photocatalysts allows the membrane to physically separate pollutants through filtration and in the presence of photocatalytic degradation by nano photocatalysts. This research can also contribute to increasing the use of membranes in treating process water treatment rubber industry into clean water.

Acknowledgement

The project presented in this article is supported by the research unit and community service faculty of engineering Diponegoro University (UNDIP) for the approved fund, making this important research viable and effective. This research is fully funded by Strategic Research Grant, No. 3178/S/kimia/UN7.5.3.2/PP/2022.

References

[1] Fong, Y. C., Khin, A. A., Lim, C. S. "Conceptual Review and the Production, Consumption and Price Models of the Natural Rubber Industry in Selected ASEAN Countries and World Market", Asian Journal of Economic Modelling, 6(4), pp. 403–418, 2018. https://doi.org/10.18488/journal.8.2018.64.403.418

[2] Massoudineja, M, Rabori, M. M., Dehghani, M. H. "Treatment of natural rubber industry wastewater through a combination of physicochemical and ozonation processes", Journal of Advances in Environmental Health Research, 3(4), pp. 243–249, 2015. [online] Available at: https://jaehr.muk.ac.ir/article_40208_f3176bd4afe68bd82b39703730a32863.pdf [Accessed: 23 November 2023]

[3] Rosman, N. H., Nor Anuar, A., Othman, I., Harun, H., Sulong, M. Z., Elias S. H., Mat Hasan, M. A. H., Chellapan, S., Ujang, Z. "Cultivation of aerobic granular sludge for rubber wastewater treatment", Bioresource Technology 129, pp. 620–623, 2013. https://doi.org/10.1016/j.biortech.2012.12.113

[4] Gaol, E. R. L., Nasir, S., Hermansyah, H., Mataram, A. "Rubber Industry Wastewater Treatment Using Sand Filter, Bentonite and Hybrid Membrane (UF-RO)", Sriwijaya Journal of Environment, 4(1), pp. 14–18, 2019. https://doi.org/10.22135/sje.2019.4.1.14

[5] Saleh, T. A., Gupta, V. K. "Chapter 1 - An Overview of Membrane Science and Technology", In: Nanomaterial and Polymer Membranes: Synthesis, Characterization, and Applications, Elsevier, 2016, pp. 1–23. ISBN 978-0-12-804703-3 https://doi.org/10.1016/B978-0-12-804703-3.00001-2

[6] Virga, E., Žvab, K., de Vos, W. M. "Fouling of nanofiltration membranes based on polyelectrolyte multilayers: The effect of a zwitterionic final layer", Journal of Membrane Science, 620, 118793, 2021. https://doi.org/10.1016/j.memsci.2020.118793

[7] Kusworo, T. D., Kumoro, A. C., Yulfarida, M. "A new visible-light driven photocatalytic PVDF-MoS_2@WO_3 membrane for clean water recovery from natural rubber wastewater", Journal of Water Process Engineering, 52, 103522, 2023. https://doi.org/10.1016/j.jwpe.2023.103522

[8] Saleem, H., Zaidi., S. J. "Nanoparticles in reverse osmosis membranes for desalination: A state of the art review", Desalination, 475, 114171, 2020. https://doi.org/10.1016/j.desal.2019.114171

[9] Yan, M., Wu, Y., Liu, X. "Photocatalytic nanocomposite membranes for high-efficiency degradation of tetracycline under visible light: An imitated core-shell Au-TiO_2-based design", Journal of Alloys and Compounds, 855, 157548, 2021. https://doi.org/10.1016/j.jallcom.2020.157548

[10] Toledo-Camacho, S. Y., Rey, A., Maldonado, M. I., Llorca, J., Contreras, S., Medina, F. "Photocatalytic hydrogen production from water-methanol and -glycerol mixtures using Pd/TiO_2(-WO_3) catalysts and validation in a solar pilot plant, International Journal of Hydrogen Energy", 46(73), pp. 36152–36166, 2021. https://doi.org/10.1016/j.ijhydene.2021.08.141

[11] Ahamad, T., Naushad, M., Alzaharani, Y., Alshehri, S. M. "Photocatalytic degradation of bisphenol-A with g-C_3N_4/MoS_2-PANI nanocomposite: Kinetics, main active species, intermediates and pathways", Journal of Molecular Liquids, 311, 113339, 2020. https://doi.org/10.1016/j.molliq.2020.113339

[12] Wang, C., Zhang, X., Yuan, B., Wang, Y., Sun, P., Wang, D. "Multi-heterojunction photocatalysts based on WO_3 nanorods: Structural design and optimization for enhanced photocatalytic activity under visible light", Chemical Engineering Journal, 237, pp. 29–37, 2014. https://doi.org/10.1016/j.cej.2013.10.003

[13] Singla, S., Sharma, S., Basu, S. "MoS_2/WO_3 heterojunction with the intensified photocatalytic performance for decomposition of organic pollutants under the broad array of solar light", Journal of Cleaner Production, 324, 129290, 2021. https://doi.org/10.1016/j.jclepro.2021.129290

[14] Pei, Z.-Z., Liu, Y.-B.. Jia, H., Zhou, J.-X., Li, F., Wang, X., He, X.-H. "Controllable Synthesis of Flower-Like MoS_2 and Its Quick Photodegradation of Methylene Blue Under Visible Irradiation", Journal of Nanoscience and Nanotechnology, 20(5), pp. 3013–3018, 2020. https://doi.org/10.1166/jnn.2020.17464

[15] Kusworo, T. D., Yulfarida, M., Kumoro, A. C., Sumardiono, S., Djaeni, M., Kurniawan, T. A., Othman, M. H. D., Budiyono, B. "A highly durable and hydrophilic PVDF- MoS_2/WO_3-PVA membrane with visible light driven self-cleaning performance for pollutant-burdened natural rubber wastewater treatment", Journal of Environmental Chemical Engineering, 11(2), 109583, 2023. https://doi.org/10.1016/j.jece.2023.109583

[16] Kusworo, T. D., Dalanta, F., Aryanti, N., Othman, N. H. "Intensifying separation and antifouling performance of PSf membrane incorporated by GO and ZnO nanoparticles for petroleum refinery wastewater treatment", Journal of Water Process Engineering, 41, 102030, 2021. https://doi.org/10.1016/J.JWPE.2021.102030

[17] Chae, J., Lim, T., Cheng, H., Jung, W. "Modification of the surface morphology and properties of graphenke oxide and multi-walled carbon nanotube-based polyvinylidene fluoride membranes according to changes in non-solvent temperature", Nanomaterials, 11(9), 2269, 2021. https://doi.org/10.3390/nano11092269

[18] Méricq, J.-P., Mendret, J., Brosillon, S., Faur, C. "High performance PVDF-TiO_2 membranes for water treatment", Chemical Engineering Science, 123, pp. 283–291, 2015. https://doi.org/10.1016/j.ces.2014.10.047

[19] Pradhana, E. A., Elma, M., Othman, M. H. D., Huda, N., Ul-Haq, M. D., Rampun, E. L., Rahma, A. "The Functionalization Study of PVDF/TiO_2 Hollow Fibre Membranes Under Vacuum Calcination Exposure", Journal of Physics: Conference Series, 1912, 012035, 2015. https://doi.org/10.1088/1742-6596/1912/1/012035

[20] Pourjafar, S., Rahimpour, A., Jahanshahi, M. "Synthesis and characterization of PVA/PES thin film composite nanofiltration membrane modified with TiO_2 nanoparticles for better performance and surface properties", Journal of Industrial and Engineering Chemistry, 18(4), pp. 1398–1405, 2012. https://doi.org/10.1016/j.jiec.2012.01.041

[21] Struzyńska-Piron, L., Bilad, M. R., Loccufier, J., Vanmaele, L., Vankelecom I. F. J. "Influence of UV curing on morphology and performance of polysulfone membranes containing acrylates", Journal of Membrane Science, 462, pp. 17–27, 2014. https://doi.org/10.1016/j.memsci.2014.03.013

[22] Wang, K., Abdalla, A. A., Khaleel, M. A., Hilal, N., Khraisheh, M. K. "Mechanical properties of water desalination and wastewater treatment membranes", Desalination, 401, pp. 190–205, 2017. https://doi.org/10.1016/j.desal.2016.06.032

[23] Hu, H., Ji, H.-F., Sun, Y. "The effect of oxygen vacancies on water wettability of a ZnO surface", Physical Chemistry Chemical Physics, 15(39), pp. 16557–16565, 2013. https://doi.org/10.1039/c3cp51848e

[24] Bibi, S., Ahmad, A., Anjum, M. A. R., Haleem, A., Siddiq, M., Shah, S. S., Kahtani, A. A. "Photocatalytic degradation of malachite green and methylene blue over reduced graphene oxide (rGO) based metal oxides (rGO-Fe_3O_4/TiO_2) nanocomposite under UV-visible light irradiation", Journal of Environmental Chemical Engineering, 9(4), 105580, 2021. https://doi.org/10.1016/j.jece.2021.105580

[25] Qin, A., Li, X., Zhao, X., Liu, D., He, C. "Engineering a Highly Hydrophilic PVDF Membrane via Binding TiO_2 Nanoparticles and a PVA Layer onto a Membrane Surface", ACS Applied Materials & Interfaces, 7(16), pp. 8427–8436, 2015. https://doi.org/10.1021/acsami.5b00978

[26] Xu, Z., Wu, T., Shi, J., Teng, K., Wang, W., Ma, M., Li, J., Qian, X., Li, C., Fan, J. "Photocatalytic antifouling PVDF ultrafiltration membranes based on synergy of graphene oxide and TiO_2 for water treatment", Journal of Membrane Science, 520, pp. 281–293, 2016. https://doi.org/10.1016/j.memsci.2016.07.060

[27] Kusworo, T. D., Kumoro, A. C., Aryanti, N., Utomo, D. P., Hasbullah, H., Lingga, F. F., Widiastuti, A., Yulfarida, M., Dalanta, F., Kurniawan, T. A. "Photocatalytic antifouling nanohybrid polysulfone membrane using the synergetic effect of graphene oxide and SiO_2 for effective treatment of natural rubber-laden wastewater", Journal of Membrane Science, 657, 120663, 2022. https://doi.org/10.1016/j.memsci.2022.120663